Metal enrichment in lithologically complex black shales: a case study from the Tremadocian of NE Estonia

Rutt Hints, Siim Pajusaar, Kristjan Urtson, Merlin Liiv and Toivo Kallaste

Department of Geology, Tallinn University of Technology, Ehitajate tee 5, 19086 Tallinn, Estonia; rutt.hints@taltech.ee, siim.pajusaar@taltech.ee, kristjan.urtson@taltech.ee, merlin.liiv@taltech.ee, toivo.kallaste@taltech.ee

Abstract. Significantly elevated U, Mo, Zn and Pb contents characterize the Early Ordovician black shales in the Sillamäe area, NE Estonia. The presence of silty interlayers with sulphidic mineralization and authigenic carbonates suggests unique physicochemical conditions for metal enrichment in this location. We investigated metallogenesis of these shallow-water black shales based on high-resolution mapping of element distribution in the Sõtke drill core and nearby Päite outcrop using X-ray fluorescence spectroscopy, inductively coupled plasma mass spectrometry and organic elemental analysis, complemented by optical microscopy and scanning electron microscopy of selected samples. Enriched metals in the black shales of the study area show dissimilar distribution trends with sharp vertical concentration gradients. The recorded variance ranges were 88–275 ppm for U, 70–2467 ppm for Mo, 85–1600 ppm for V, 21–17 283 ppm for Zn and 95–26 549 ppm for Pb, while total organic carbon varied from 0.5 to 13 wt%. In most cases, the metals showed no clear covariance with organic matter or other major compounds such as S or P. The development of a sulphate reduction zone near the sediment–water interface with a sharp decrease in Eh, production of H_2S, elevated alkalinity and pH, and (re)distribution of phosphorus probably controlled the syngenetic capture of Mo and U. Enhanced transfer of fluids and solutes in coarse-grained permeable beds facilitated the accumulation of metals, while the deposit probably acted as a semi-open geochemical system throughout its geological evolution. Local Zn and Pb enrichment developed due to the intrusion of late diagenetic metal-bearing fluids and the entrapment of metals in beds that contained authigenic carbonates.

Key words: black shale, metals, phosphate, sulphate reduction, Ordovician, graptolite argillite.

INTRODUCTION

Tremadocian metalliferous and organic-rich black shales of the Türisalu Formation (commonly referred to by local names 'graptolite argillite' or 'Dictyonema shale') from the Early Palaeozoic sedimentary succession of Estonia have recently attracted new interest as a potential future source of rare metals for high-tech industry (Hade & Soesoo 2014). Although studied for almost two centuries since Eichwald (1840), the details of the metallogenesis of these U–Mo–V-rich black shales are still poorly understood, including the factors that led to the development of spatiotemporal variance of enriched metal assemblages.

The syngenetic trapping of redox-sensitive and chalcophile metals from oxygen-deprived seawater is widely considered to be the main pathway for metal enrichment in black shales, as low oxygen fugacity and high organic matter (OM) content promote their syngenetic accumulation in fine-grained sediments. The degree of enrichment of redox-sensitive elements, such as U, Mo or V, has been shown to be a useful palaeoredox proxy for interpreting the occurrence of anoxic or euxinic conditions in palaeoseawater (Jones & Manning 1994; Algeo & Maynard 2004; Tribovillard et al. 2006; Scott & Lyons 2012). However, such enrichment models, which build on the variations of Eh in the primary water column, cannot explain the genesis of particularly enriched metal horizons or zones in black shales. In such cases, additional factors, e.g. intermittent euxinia, dynamic sedimentation processes, enhanced metal transfer, microbial reduction or influence of hydrothermal solutions, might have had ultimate control over metal accumulation (e.g., Coveney & Nansheng 1991; Schovsbo 2002; Johnson et al. 2017). A better understanding of the mechanisms behind the development of such above-average metal enrichment in black shales could facilitate the further discovery of potentially exploitable resources within extensive black shale complexes (e.g., Pagès et al. 2018).

The present study addresses the possibility that the significant metal enrichment of the lithologically heterogeneous shallow-water Tremadocian black shales was controlled by the physical characteristics of the sediment and the formation of an effective (bio)geochemical trap within the deposit. The metalliferous black shales are mostly considered to have evolved via closed geochemical systems after initial syngenetic enrichment. Nevertheless, recent studies of contemporaneous Tremadocian black shales of the nearby St Petersburg region suggest that these beds might have evolved under more open geochemical systems with possible mobilization of redox-sensitive U as a result of the influx of glacier meltwater during the last ice age (Schulz et al. 2019). Thus, mass exchange processes might have played a more crucial role in the development of metal enrichment patterns in these black shales compared to more lithologically homogeneous mudstone sequences.

This study is based on high-resolution sampling and geochemical investigations of black shale profiles in the Sillamäe area. In that area the black shale pilot mine and U-enrichment plant operated for a short period in the 1950s (Lippmaa et al. 2011).

GEOLOGICAL SETTING AND SITE DESCRIPTION

The studied black shales belong to the once laterally extensive, but now only sporadically preserved Cambrian–Lower Ordovician black shales of the epicontinental Baltic Palaeobasin (Fig. 1A) (Andersson et al. 1985; Heinsalu & Bednarczyk 1997). This extensive and flat-bottomed basin was characterized by intensive upwelling in parts facing the Iapetus Ocean (Wilde et al. 1989) and by extremely limited input of siliciclastic material from terrestrial areas (Felitsyn et al. 1998; Artyushkov et al. 2000; Sturesson et al. 2005) in the Early Ordovician. The territory of Estonia and the St Petersburg district (Russia) comprised a shallow-water peripheral portion of the basin at that time (Artyushkov et al. 2000; Nielsen & Schovsbo 2006).

In Estonia, thermally immature (Kirsimäe et al. 1999) siliciclastic-carbonate sedimentary rocks of the Lower Palaeozoic and Ediacaran overlie the highly tectonized and metamorphosed Proterozoic basement (Puura & Vaher 1997). The maximum thickness of the Türisalu Formation (~7 m) is reached in NW Estonia and decreases from there east- and southwards (Fig. 1B). The burial depth of the complex varies from 0 m to more than 250 m. The black shales that form the Türisalu Formation were deposited above the coastal and shallow-marine siliciclastic complexes and are rich in biogenic phosphatic detritus (Fig. 1C). High phosphorus-loading and elevated primary productivity are considered to be characteristic features of the Early Ordovician Baltic Palaeobasin (Leventhal 1983; Wilde et al. 1989; Baturin & Ilyin 2013). The non-contemporaneous nature of the transgressive black shale beds (Kaljo & Kivimägi 1970), which recorded high spatiotemporal variations in sedimentary fabrics and dynamic deposition and erosion structures, as well as the common presence of silty interlayers, suggest that the mud accumulated in relatively shallow-water settings (Hints et al. 2014).

K-feldspars, quartz and illitic illite-smectite/mica form the dominant part of the mineral matrix in these organic-rich and sulphidic black shales (Utsal et al. 1980; Loog et al. 2001). The youngest part of the Türisalu Formation remaining in the Sillamäe area contains the highest proportion of coarse-grained material (Loog et al. 2001). Pyrite is predominant among the sulphidic minerals. Its content varies from 4% to 6%, and it is omnipresent as disseminated microcrystalline forms (Kallaste & Pukkonen 1992). In siliciclastic interlayers, pyritic or more rarely polymetallic mineralization with marcasite, sphalerite and galena sporadically occur (Petersell et al. 1987). The presence of Mo-, U- and V-minerals has not been unequivocally identified in the Türisalu Formation. These metals are assumed to occur predominantly in the form of metal–organic compounds (Petersell 1997) such as porphyrins (Lippmaa et al. 2009) or via complexes with humic acids (Bogdanov et al. 2007). Few studies suggest the presence of U-rich biogenic and authigenic apatite (Kochenov & Baturin 2002) and possibly uraninite (Bogdanov et al. 1994). Pukkonen (1989) divided the Türisalu Formation into three lateral geochemical zones (Fig. 1B) based on metal enrichment patterns, with the third geochemical zone being especially rich in elements typically associated with sulphides and phosphates, such as U and Mo (Hade & Soesoo 2014).

The samples used for this study come from the Sõtke 1 drill core (WGS84 coordinates: 59° 22.38′, 27° 42.47′) near the town of Sillamäe (Fig. 1D). The borehole was drilled by the Geological Survey of Estonia (Karimov et al. 2017) as a part of a project for investigating the bioleaching potential of the black shales of the Türisalu Formation. On the basis of historical data, the borehole was targeted to the zone of the highest mineralization grades in the Türisalu Formation. Earlier drill sections of the Türisalu Formation from NE Estonia had not been preserved or were in a too deteriorated state as a result of sulphide oxidation and disassociation of loosely cemented silty interbeds.

The total thickness of the Türisalu Formation in the Sõtke borehole is ~1.1 m. However, the core recovery for the Türisalu Formation was only 50%, and a considerable part from the lower half of the section is missing. An image of the black shale section of the Sõtke core is provided in the electronic supplement available at
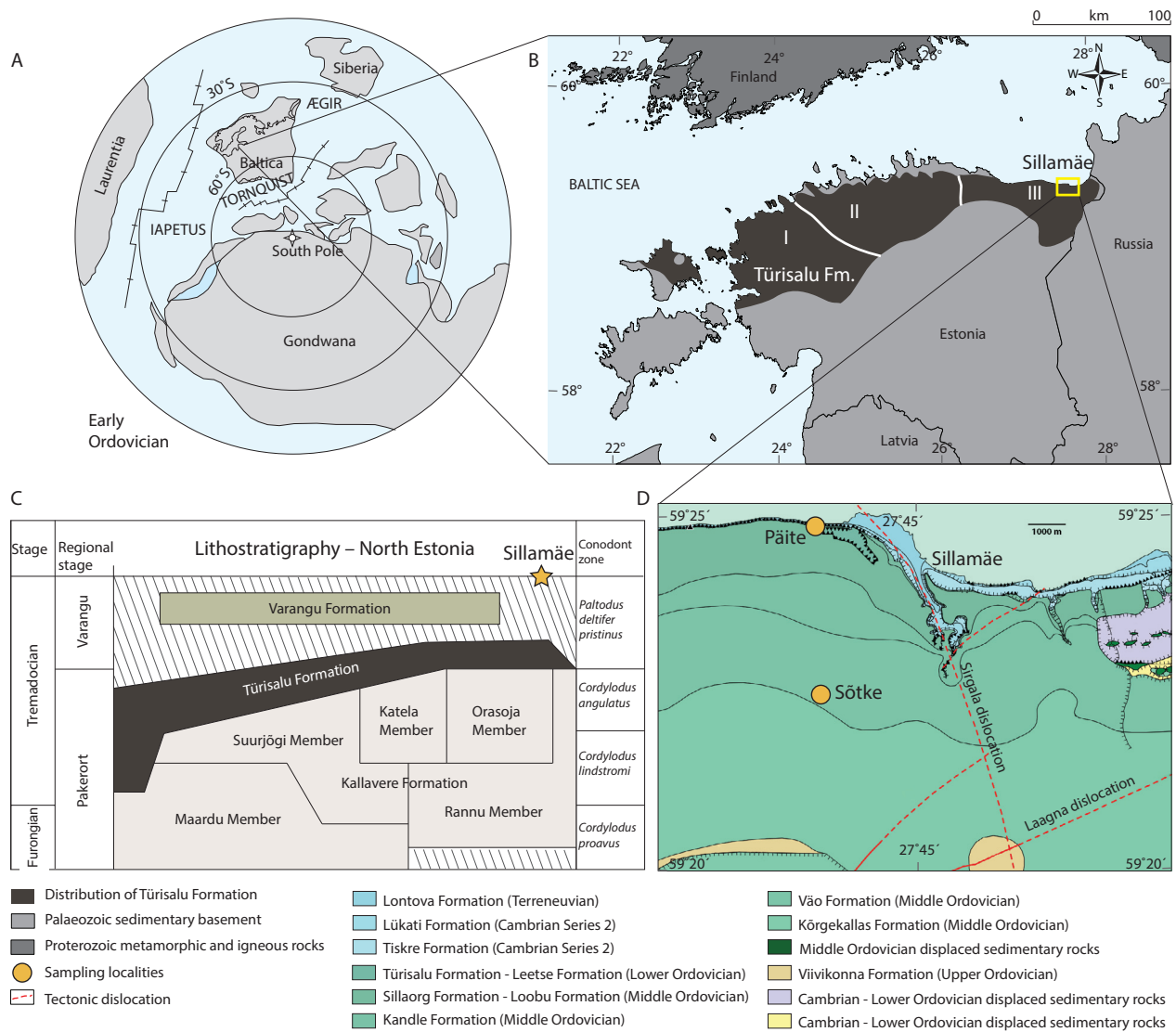
Fig. 1. A, position of Baltica and the Baltic Palaeobasin in the Early Ordovician, after Cocks & Torsvik (2006). **B**, distribution of Tremadocian black shales (Türisalu Formation) in the territory of Estonia; Roman numbers mark different geochemical zones of the black shales, according to Pukkonen (1989). **C**, lithostratigraphic schema of the Türisalu Formation in North Estonia along the west–east directed profile after Heinsalu et al. (2003). **D**, geological map with studied localities near Sillamäe (base map from Estonian Land Board online map services).

https://doi.org/10.15152/GEO.500. Also, composite samples from the nearby Päite Klint section (WGS84 coordinates: 59° 24.86′, 27° 42.12′) collected by the Geological Survey of Estonia were analysed for the study. The thickness of the Türisalu Formation in the Päite Klint section is ~1.2 m. The klint section was sampled via two intervals, from 0 to 0.7 m and from 0.7 to 1.2 m below the upper contact of the Türisalu Formation. For sampling, ~15 cm of weathered black shale was first removed from the outcrop surface. The black shales were then sampled along a vertical trench by hammering. For both intervals, approximately 40 kg of rock was collected.

METHODS

The black shale from the Sõtke core was sampled at 2-cm intervals along the entire length of the profile using a quarter of the core. The samples were then crushed and milled with a tungsten carbide mill. Elemental analyses

of bulk samples were conducted at the Department of Geology, Tallinn University of Technology. The Geological Survey of Estonia conducted the crushing and homogenization of composite samples from the Päite Klint and reduction to the testing size by the quartering. X-ray fluorescence spectroscopy (XRF) and inductively coupled plasma mass spectrometry (ICP-MS) were used to measure the content of major and trace elements in bulk samples. For XRF analyses, 8 g of powder was pressed into a pellet and then analysed with a Bruker S4 spectrometer using Bruker's precalibrated MultiRes measurement method. The in-house reference sample ES2 (Kiipli et al. 2000) was used for calibration. The ES2 reference sample is composed of material from the black shale of the Türisalu Formation. It has been regularly used for black shale and oil shale studies, along with external standards to ensure the analytical quality of the labs. For ICP-MS studies, a mixture of 0.1 g of the sample and 1.0 g of lithium metaborate (49.75%), lithium tetraborate (49.75%) and lithium bromide (0.50%) flux was fused in a platinum crucible and subsequently dissolved in a solution of 7% nitric acid and 2% hydrochloric acid. Solutions were diluted and placed into a Thermo X-series II ICP-MS instrument that was calibrated using multielement reference solutions (Inorganic Ventures Inc.). Total organic carbon (TOC) content was measured through combustion in a FLASH 2000 Organic Elemental Analyzer, as follows. Approximately 8 mg of dried powdered sediment was placed into silver containers, having been initially pre-treated with 10% HCl, dried on a hotplate at 80 °C for 5 h and left to cool. Before analysis, the silver containers were packed into tin containers to facilitate combustion. Cystine was used as a standard (ThermoFisher Scientific) and organic-rich sediment was used as reference material (IVA Analysentechnik e.K.). Polished samples and thin sections from selected intervals of black shales from the Sõtke core were prepared and examined by optical microscopy. Uncoated thin sections were studied with a Zeiss EVO MA15 scanning electron microscope using a backscattered electron detector, while an Oxford INCA energy-dispersive detector was used for microanalyses and identification of mineral phases, by applying a beam accelerating voltage of 20 kV.

To compare the recorded trace element enrichment values with those reported from other organic-rich sedimentary rocks, the element content (X) was normalized with respect to the aluminium concentration in the sample and the enrichment factor (EF) was calculated according to the formula (e.g., Algeo & Maynard 2004)

$$X_{EF} = [\left(\frac{X}{Al}\right)_{sample} / \left(\frac{X}{Al}\right)_{PAAS}], \qquad (1)$$

where X_{PAAS} and Al_{PAAS} represent respective element values in the post-Archaean average shale (PAAS) composite (Taylor & McLennan 1985).

RESULTS

Sedimentary fabrics and mineral characteristics

Black shales from the Sõtke core section were characterized by abrupt changes in grain size and porosity. The section of black shale in the Sõtke core consisted of organic mudstone layers intercalated by silty interlayers in the lower part of the profile (an interval which showed rather poor core recovery). According to the drilling report (Karimov et al. 2017), this interval was set apart by the occurrence of sandy/silty beds with a thickness of 2–3 cm. The documented features comply with descriptions of the lower part of the Türisalu Formation provided by previous studies of the Türisalu Formation in the area of interest (e.g., Heinsalu et al. 2003). Loosely consolidated sandy/silty intervals were probably preferentially lost during drilling. These poorly sorted black shales frequently demonstrated normal grading, erosional bedding surfaces indicative of dynamic deposition environment, open macroporosity and calcite fillings within organic particles (Fig. 2A) (e.g., Hints et al. 2014).

Striped black shales consisting of thin intercalated black shale laminae and strongly sulphidic silty interlayers made up the middle part of the profile. The horizon was characterized by fine-grained and finely horizontally laminated mudstone. In silty interlayers pyrite and calcite occurred as the main cementing phases. This interval probably represents the most condensed section of the black shale complex deposited during the maximum marine flooding stage. The formation of abundant pore-filling iron sulphides in this interval could be an indicator of slow sedimentation rates, which would have allowed the accumulation of enough iron for iron-sulphite precipitation due to reworking of underlying sediments (e.g., Schieber & Riciputi 2005) or due to particle shuttles of Fe (e.g., Dellwig et al. 2010).The upper part of the black shale complex was characterized by the presence of various forms of authigenic carbonates (sparry, bladed and microgranular) and pyrites (frequently detected in close association with the carbonate aggregates) and lenses of microcrystalline quartz with poorly preserved spicules of silica sponges. The black shales in this upper part of the complex showed a gradual change towards less sorted varieties. The interval also presented common soft sediment deformation of the surrounding mudstone around calcite aggregates, indicating that the growth of aggregates occurred in rather poorly consolidated mud.
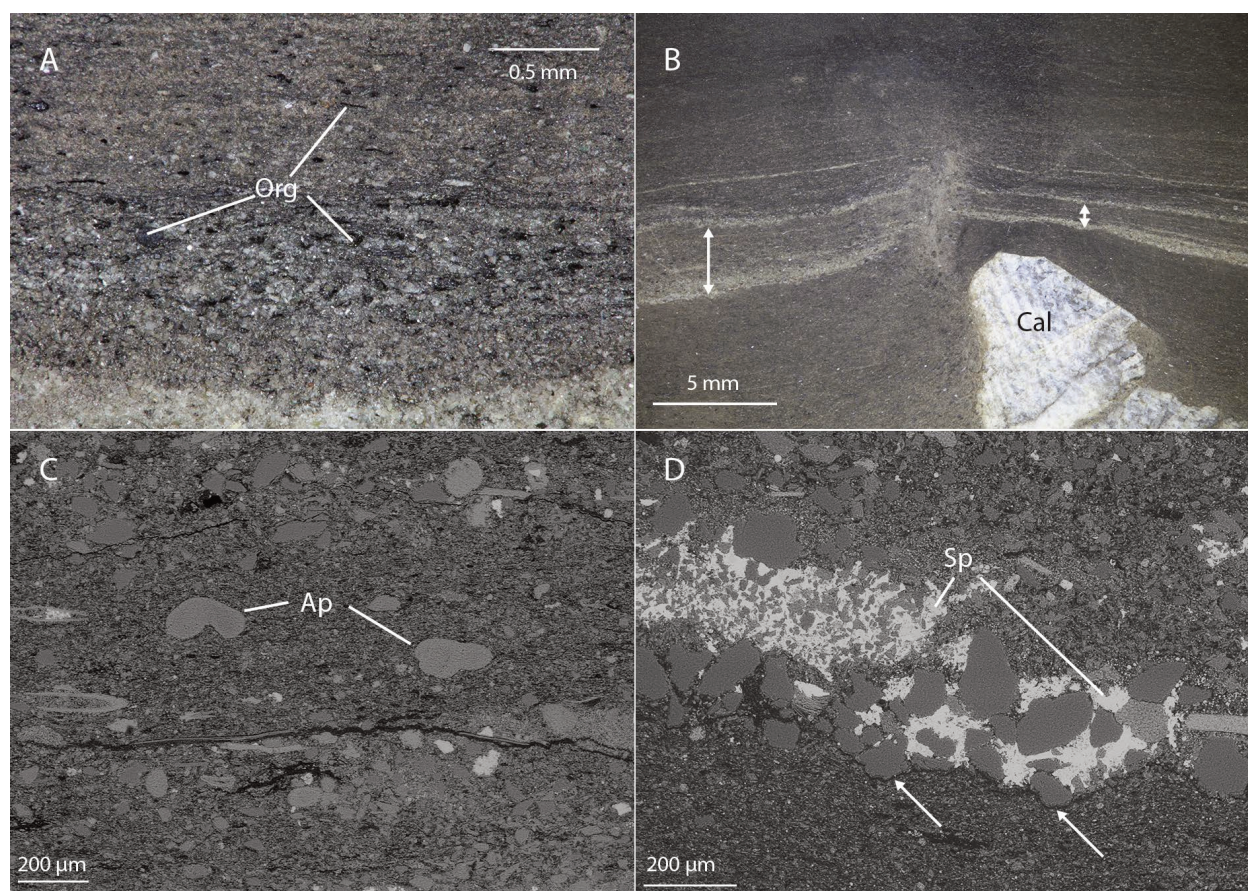
Fig. 2. Examples of microstructures and authigenic phases in black shales from the Sõtke core. **A**, **B**, images of polished cuts obtained with stereomicroscope. A, poorly sorted black shale from the lower part of the Sõtke core, showing partly opened macroporosity. Refractory organic particles preserved in 3D shape contain calcite fillings. B, soft sediment deformation produced by gas or fluid escape from black shale simultaneously with the growth of authigenic carbonate. The black shale from the upper part of the Türisalu Formation. Note the different compaction of the black shale lamina above calcite spar (arrows), hinting at carbonate growth in poorly consolidated mud. **C**, **D**, backscattered scanning electron microscope image of thin sections. C, authigenic globular phosphate aggregates in poorly sorted black shale from the upper part of the Sõtke profile. D, sphalerite crystals infilling pore space of a silty lens above a stylolitic bedding surface (arrows), sampled from the upper part of the Sõtke profile. Abbreviations: Org, particulate organic matter; Cal, calcite; Ap, apatite; Sp, sphalerite.

Other observed soft sediment deformations included features suggestive of fluid or gas seepage (Fig. 2B). Considering that larger pyritic aggregates, as well as fillings from overlying laminae, were detected along such deformations, these features apparently acted as important pathways for mass transport in the mud beds.

Analyses by SEM-energy dispersive spectrometer (SEM-EDS) confirm the presence of calcite and iron sulphides as the major phases of authigenic macro-crystalline aggregates and pore fillings in the siliciclastic beds. Calcium phosphates occurred in the studied samples as bioclastic apatite (conodonts); however, the phosphate phases in the upper part of the Sõtke profile were also present in the form of numerous small authigenic spherulitic aggregates (Fig. 2C). Microanalyses revealed the occurrence of irregular lamina-bound sphalerite mineralization in the uppermost part of the Sõtke section. Sphalerite mostly occurring via pore filling in lenses within coarse-grained poorly sorted black shale laminae was clearly associated with stylolitic bedding surfaces in some cases (Fig. 2D).

Major elements and TOC

The main geochemical characteristics of the studied samples are summarized in Table 1 and illustrated in Fig. 3. The full geochemical dataset for the black shales of the Sõtke core is provided as an electronic supplement at

Table 1. Concentrations of selected elements, total organic carbon (TOC) and geochemical characteristics in samples of the Türisalu Formation

	Sõtke drill core						Päite outcrop*	1st zone**		2nd zone**	
	n = 29						n = 2	n = 258		n = 25	
	min	max	mean	std	skew	kurtosis	mean	mean	std	mean	std
TOC (wt%)	0.5	13.1	7.2	3.4	–0.2	–0.5	5.7	10.0	2.27	8.5	2
S (wt%)	1.2	24.1	4.3	4.9	3.3	11.0	6.6	3.3	1.2	3.3	1.5
Al_2O_3 (wt%)	2.0	13.2	9.9	2.9	–1.2	0.9	4.5	11.3	1.6	11.5	1.8
TiO_2 (wt%)	0.1	0.8	0.5	0.2	–1.1	0.6	0.5	0.7	0.1	0.7	0.1
P_2O_5 (wt%)	0.1	6.6	1.5	1.8	2.2	4.1	1.0	0.2	0.2	0.2	0.2
CaO (wt%)	0.2	37.7	6.8	8.5	2.2	5.6	3.8	0.9	2.98	0.9	1.9
Fe_2O_3 (wt%)	2.1	45.0	8.0	9.1	3.5	11.9	9.9	4.9	1.68	5.0	0.9
V (ppm)	85	1600	1004	360	–0.6	–0.5	850	1035	289	640	226
Zn (ppm)	21	17283	2657	4192	2.2	14.1	348	206	671	62	36
Mo (ppm)	70	2467	509	514	2.3	6.7	303	189	94	104	101
Pb (ppm)	95	26549	1152	4880	5.3	28.6	191	126	41	102	30
U (ppm)	88	732	275	192	1	–0.03	238	111	39	61	40
TREE (ppm)***	44	634	296	152	0.4	–0.3	436	196	50	199	54
V/TOC (ppm/wt%)			131				150	104		76	
Mo/TOC (ppm/wt%)			67				53	19		12	
U/TOC (ppm/wt%)			36				42	11		7	
V/Al (ppm/wt%)			184				189	173		106	
Mo/Al (ppm/wt%)			95				69	32		17	
U/Al (ppm/wt%)			55				53	18		10	

* composite samples representing the lower and upper parts of the black shale profile, ** content of selected elements and TOC from the first and second geochemical zones from Vind & Bauert (2020), ***total rare earth element content

https://doi.org/10.15152/GEO.499. It should be noted that the reported whole-rock data included samples with mixed lithologies containing both black shales and (sulphidic) siliciclastic laminae. The studied black shales have a considerably low average TOC content (7.2 ± 3.4 wt%) and high average content of Ca (6.8 ± 8.5 wt%), P (1.5 ± 1.8 wt%), S (4.3 ± 4.9 wt%) and Fe_2O_3 (8.1 ± 9.1 wt%) compared to mean values recorded in the first and second geochemical zones of the Türisalu Formation (Pukkonen 1989; Vind & Bauert 2020). Nevertheless, high-resolution vertical geochemical patterns in the black shales demonstrate significant sample-to-sample variance and specific changes in particular horizons (Fig. 3). Thus, the highest Fe and S contents were recorded within the condensed stripped black shale interval in the middle of the Sõtke core. Particularly, P-rich black shales characterize the uppermost poorly sorted portion of the Türisalu Formation (the interval which contains authigenic

phosphates). Nevertheless, the Ti/Al ratios calculated for the Sõtke sections were relatively constant over the whole profile ($6.2 \pm 0.4 \times 10^{-2}$), interpreted to reflect invariable input of terrigenous matter from the same source area. The strong positive correlation detected between Al and TOC values ($R^2 = 0.80$, $n = 29$) indicates that black shale varieties with a higher aluminosilicate content tended to contain higher proportions of OM.

Enriched metals

The values of U and Mo in the black shales of the Sillamäe area invariably revealed more than 10-fold enrichment compared to the crustal averages (Taylor & McLennan 1985) and a significant enrichment compared to the average values of the black shales of the Türisalu Formation in other geochemical zones (Vind & Bauert 2020; Table 1). The calculated element enrichment factors
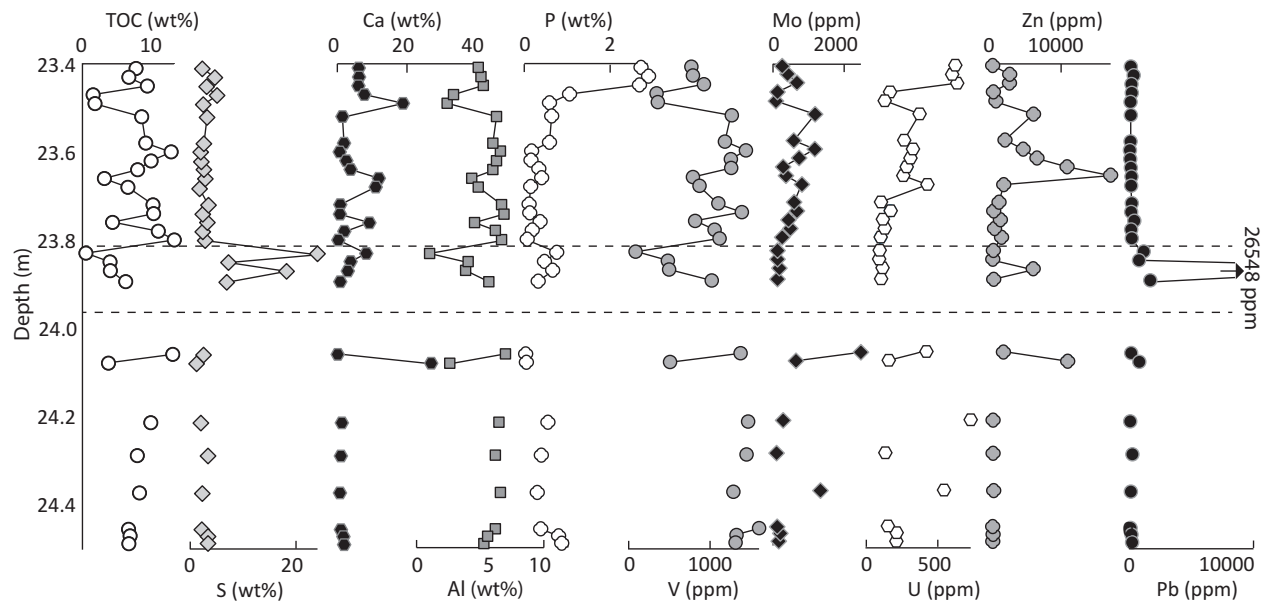
Fig. 3. Compositional trends of enriched metals and selected compounds in the black shales of the Sõtke core. Trend lines are shown only for the portion of the profile for which mostly continuous core section recovery could be assumed. Dotted lines mark boundaries between lithological varieties of the black shale: the lower transgressive varigrained part of the Türisalu Formation, stripped black shale unit, the upper part of the Türisalu Formation.

for U, Mo, V and Zn varied in a wide range, with Mo_{EF} reaching >1000 in several samples and U_{EF} > 100 in more than half of the samples. In contrast, Zn showed fluctuations from strongly enriched (EF > 100) to non-enriched (EF = 1) levels.

As indicated by the geochemical record of the Sõtke section, each enriched element possessed a different distribution pattern (Fig. 3) and the maximum enrichment of the elements was related to different horizons. Molybdenum was on average several-fold enriched in samples from the Sillamäe area compared to the same complexes from West and middle North Estonia. The calculated Mo_{EF} values for the Sõtke core section varied from 147 to 3570. Molybdenum distribution showed a rather weak positive correlation with TOC ($R^2 = 0.29$, $n = 29$) (Fig. 4). Notably, Mo did not demonstrate any systematic variance with respect to Fe or S content. The V_{EF} value ranged from 6 to 18. Vanadium distribution was biased towards higher values and strongly positively correlated with those of Al ($R^2 = 0.80$, $n = 29$) and Ti ($R^2 = 0.86$, $n = 29$), and moderately strongly with that of TOC ($R^2 = 0.60$, $n = 29$). Uranium in the studied samples showed more than two-fold enrichment compared to other geochemical zones, with U_{EF} varying from 47 to 381. Uranium did not present meaningful covariance with TOC or other major compounds such as P. Nevertheless, in the upper horizon of the Sõtke core, an anomalously high content of U appears together with an elevated P content and in the

presence of authigenic calcium phosphates. The phosphate distribution in the Sõtke black shales exhibited a very strong correlation with the abundance of total rare earth elements (REE) ($R^2 = 0.88$, $n = 26$) if outlier values in the upper U-phosphate-rich samples were excluded. As REE demonstrate a very strong affinity for phosphate phases, such variance likely indicates that phosphogenesis in these U-phosphate-rich varieties differed from the rest of the deposit. One should notice that due to poor core recovery, the geochemical dataset of the Sõtke core is not representative for the lower part of the Türisalu Formation. According to the natural gamma-ray downhole survey of the Sõtke borehole (Karimov et al. 2017), natural gamma radioactivity in the lower part of the Türisalu Formation showed similar values to the upper part, suggesting similar U-enrichment levels for both intervals.

Zinc and Pb in the Sõtke core showed exceptionally high concentrations compared to the average values reported in the first and second geochemical zones, but also remarkably high variance ranges. The distribution of Zn was strongly biased towards lower values and higher-grade mineralization was localized to thin horizons. In the case of Pb, a single sulphidic silty horizon in the stripped black shales interval produced an extremely high concentration. In the Sõtke core, the Zn values were highest in samples with the highest Ca content and containing authigenic carbonates. Furthermore, composite samples
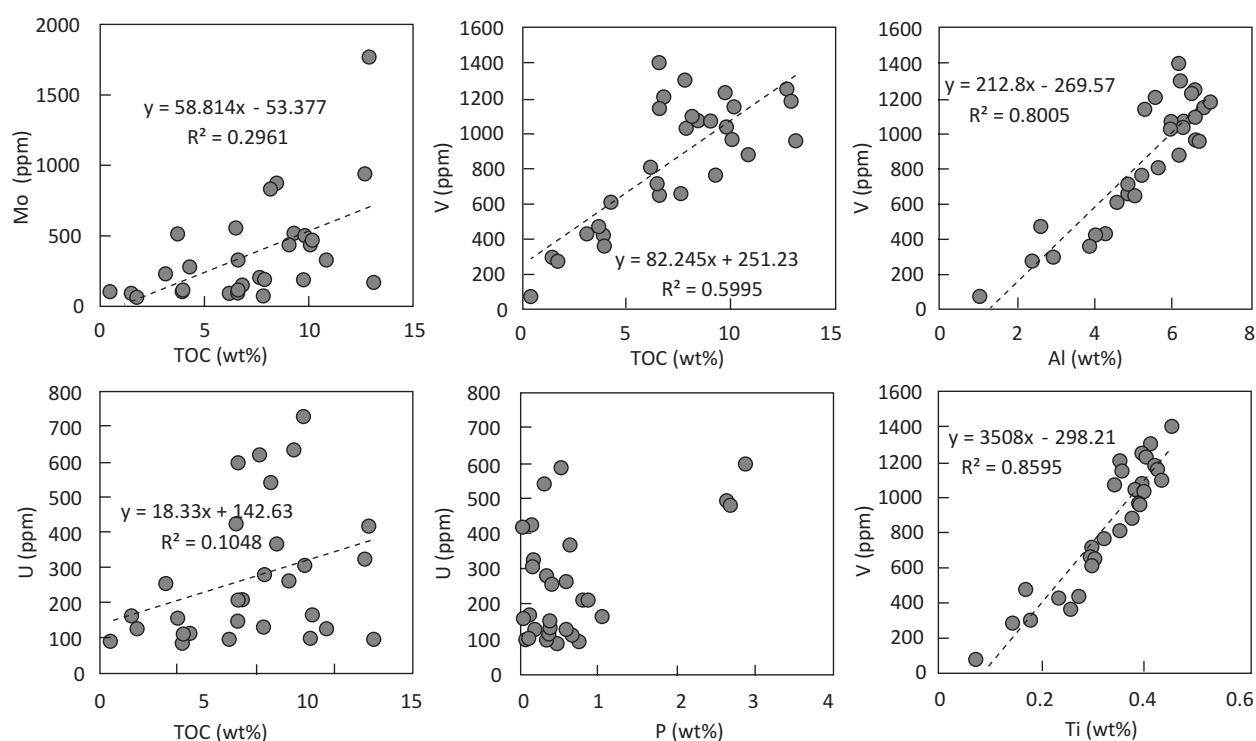
Fig. 4. Scatter plots illustrating U–TOC, Mo–TOC, V–TOC, V–Ti, U–P and V–Al relationships in the black shales of the Sõtke core.

from the Päite Klint, with a lower average Ca content, showed considerably lower average concentrations of Zn than the black shales from the Sõtke core. Missing intervals in the Sõtke section could partly explain the discrepancy of average Zn contents between two settings. Nevertheless, the Zn content of the composite sample from the upper part of the Päite Klint (577 ppm) is approximately five times lower than the average Zn content in the upper part of the Türisalu Formation of the Sõtke core.

Metallogenesis of major enriched compounds

The redox sensitive metals U, Mo and V typically exist under Earth surface conditions in multiple redox states and tend to form soluble complexes in oxic environments and low-solubility forms under anoxic conditions, therefore commonly accumulating in marine organic-rich rocks and sediments (e.g., Tyson 2001; Tribovillard et al. 2006; Smedley & Kinniburgh 2017). Anaerobic breakdown of organic compounds, including microbially mediated sulphate reduction, is widely seen as the key driver of their accumulation. Sulphate reduction processes are also critical for the behaviour of chalcophile elements such as Mo, Pb and Zn in sedimentary systems, while these elements tend to form sulphidic minerals under euxinic conditions.

On the basis of the extensive dataset from the modern and palaeomarine oxygen-deficient settings, Algeo & Tribovillard (2009) demonstrated that covariance of syngenetically enriched U and Mo might help to delineate settings with different benthic redox conditions, degree of openness of the marine basin and role of Fe–Mg shuttles. They suggested that under oxic marine conditions, the accumulation of U from seawater into sediments slightly surpasses that of Mo. In contrast, under increasingly reducing conditions and non-restricted marine basins, Mo accumulation efficiency tends to equalize with that of U. The trapping of Mo to sediments surpasses that of U if the sulphidic environment becomes prevailing (Tribovillard et al. 2006). Figure 5 demonstrates the enrichment factors of U and Mo of the studied black shale samples from the Sõtke core, with respect to molar ratios of U/Mo in modern seawater (∼7.5–7.9; Algeo & Tribovillard 2009). While for the part of samples Mo/U ratios stay between 0.3 times the seawater and normal seawater, in other cases, samples are notably enriched with respect of Mo producing Mo/U ratios, which exceed more than three times those of the average seawater. However, a total increase in enrichment is not accompanied by a decrease in Mo/U ratios as predicted for restricted basins with the permanently euxinic lower water column (Algeo & Tribovillard 2009). Despite the high dispersion of Mo/U ratios, the values are loosely clustered along with the
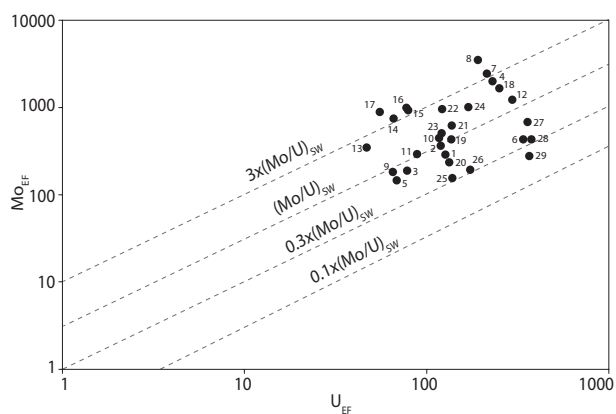
Fig. 5. U–EF vs Mo–EF diagram for the samples from the Sõtke core. The samples are numbered starting from the lowermost sample in the core section. The diagonal lines are multiples (0.3 and 3) of the Mo/U ratio of present-day seawater after Algeo & Tribovillard (2009).

normal seawater U/Mo trend, validating the general assumption that seawater was a source of the metals.

The genesis of recorded high-grade mineralization of rare metals might have been facilitated by slow deposition burial rates of the mud (e.g., Morford et al. 2007) as the long-term deposition rates of the Cambrian organic-rich muds in the Baltic Palaeobasin were extremely low (1–10 mm per 1000 years according to Thickpenny 1984). However, Schovsbo (2002) argued that more vigorous water movement at the sea bottom, rather than merely slow sedimentation rates or steady-state anoxia in water column anoxia, facilitated higher U-enrichment shore-wards in the Alum Shale. The study demonstrates the importance of sediment–water interface fluxes and characteristics in syngenetic metal enrichment in shallow organic-rich facies of the epicontinental basins.

Molybdenum

It has been shown that Mo reduction is strongly dependent on the presence of aqueous S species (Erickson & Helz 2000; Smedley & Kinniburgh 2017). Under aerobic conditions, Mo(VI) can be adsorbed by Fe- and Mn-(oxy)hydroxides (Algeo & Lyons 2006) but remains less reducible than V and U under anoxic, non-sulphidic conditions. However, after an increase in aqueous H_2S above critical threshold levels (~10 μM), Mo forms highly particle-reactive thiomolybdates (Helz et al. 1996) and can then be rapidly sequestrated to an organic fraction and precipitate via Mo-containing sulphides (Scott & Lyons 2012). Interestingly, Mo is not prominently enriched with respect to U in the most sulphide-rich pyritic condensed part of the Sõtke section. The U/Mo ratios stay constant and very close to that of average seawater (Fig. 5,

samples 9–12), signalling that metal entrapment likely occurred under an anoxic rather than euxinic water column.

The development of sulphidic and organic-rich facies in ancient epicontinental basins has been interpreted via the expansion of the basinal euxinic puddle (e.g., Wignall & Newton 2001) or oceanic oxygen minimum zone (e.g., Schlanger et al. 1987) or as a consequence of widespread euxinia in ancient oceans (e.g., Gill et al. 2011). The primary sedimentary settings of the Türisalu Formation were characterized by high P-loading and bioproductivity similar to those of modern ocean upwelling zones with common anoxia in the water column due to organic matter degradation. However, as assumed water depth was likely in a range of few tens of metres in the peripheral part of the basin (Heinsalu 1987), the flux of organic particles to the sea bottom could have been considerably higher than in ocean margins (due to a shorter sinking path of particulate matter; e.g., Helz & Vorlicek 2019). Guilbaud et al. (2017) argued, on the basis of Fe speciation in Lower to Middle Cambrian sediments of the Baltic Palaeobasin, that the distribution of oxygen-deprived facies could be explained by high bioproduction rates in those marine settings. They suggested that anoxia was locally triggered in mid-self localities, whereas a spatially restricted anoxic wedge developed that was surrounded by normally oxygenated settings. Such locally controlled and dynamic rather than steady-state euxinic conditions are consistent with the Mo-enrichment record from the Sillamäe black shales.

It has been shown that in highly productive basins, the diffusion of sulphide from the shallow pore waters could be more critical for the development of euxinic conditions in the sea bottom than *in situ* production of H_2S in the water column (Scranton et al. 1987). Molybdenum enrichment has been observed in modern anoxic–euxinic basins but also in cold seeps, where intensive anaerobic oxidation of methane with coupled dissimilatory sulphate reduction takes place near the sediment–water interface (Deng et al. 2020), creating a favourable geochemical environment for Mo entrapment. The reaction can be described by the following general equation:

$$SO_4^{2-} + CH_4 \rightarrow HS^- + HCO_3^- + H_2O. \qquad (2)$$

The reaction leads to an increase in dissolved H_2S in pore water, increased alkalinity and precipitation of authigenic carbonates. Authigenic carbonate aggregates from the Türisalu Formation revealed $\delta^{13}C$ from +0.6‰ to −8.9‰ and were presumably formed by the recrystallization of the synsedimentary metastable hydrated calcium carbonate mineral ikaite (Popov et al. 2019). Mixed carbon pools, including dissolved organic carbon from seawater as well as biogenic methane produced by carbon remineralization reactions in sediments, might have

participated in the formation of ikaite (Mikhailova et al. 2019). Importantly, sulphate reduction in shallow pore water is regarded as one of the few processes which could induce a major alkalinity shift needed for the precipitation of authigenic carbonates (besides methane some other electron donors might favour the alkalinity increase) (e.g., Zhao et al. 2016). The simultaneous decrease in TOC and increase in authigenic carbonates (inferred from high Ca content and Ca/P ratios) in the black shale of the Sõtke core is in accordance with *in situ* mineralization of OM. Black shale horizons with elevated Mo are spatially related to intervals holding authigenic carbonates. Furthermore, the average Mo content was higher in the carbonate-rich black shales of the Sõtke core than in the somewhat less Ca-rich black shales of the Päite outcrop. This difference might also be due to the alteration of outcrop samples or sampling biases rather than due to primary variations (e.g., Wilde et al. 2004).

Nevertheless, it is likely that the higher permeability of the primary mud beds, which would have allowed enhanced transport of aqueous and gaseous reactive compounds including dissolved organic compounds and SO_4^{2-} across the sediment–water interface and within sediments, allowed a well-defined intensive sulphate reduction zone to develop just below this interface. Thus, sharp redox gradients at the sediment–water interface, maintained by a high OM flux to the sea bottom, rather than steady-state water column euxinia, might have facilitated syngenetic enrichment of Mo. As dynamic and transient environmental conditions have been shown to support increased Mo accumulation in sediments (Algeo & Lyons 2006; Scholz et al. 2018), non-steady-state seepage of H_2S to seawater could also promote Mo entrapment.

Vanadium

Vanadium distribution in the Sõtke core appears to be tightly linked to the input of phyllosilicates and Ti-containing phases. According to Utsal et al. (1980), at least 10% of the fine mineral fraction of black shales of the Türisalu Formation was produced from the crystallization of volcanic ash particles. Still, this element is on average approximately seven-fold enriched in the studied black shales compared to average Post-Archaean Australian Shale values (Taylor & McLennan 1985). The V/Al ratios of the black shales exceed those of average acidic volcanic particulate matter (Schlesinger et al. 2017) by the same order of magnitude, indicating that simple input via vanadiferous detrital minerals or volcanic ash was unlikely. In the samples analysed, V also demonstrated moderately strong covariance with OM, which might imply that it was instead incorporated into organic complexes, such as metalloporphyrins (Breit & Wanty 1991), as has been suggested by some earlier studies

(Lippmaa et al. 2011). Vanadium enrichment in modern oceans occurs under highly productive water masses, enriched in dissolved P (Breit & Wanty 1991). Mobile V(V) species could be incorporated into phytoplankton biomass or be reduced to V(IV) due to low oxygen in the water column, or directly by OM, while reduction takes place under less reducing conditions compared to those for U and Mo (Algeo & Maynard 2004). Reduced V could be then scavenged by organic particles and transported into the sediment (Breit & Wanty 1991).

However, vanadate (V(IV)), which is the most widely present V species under oxic conditions, could also strongly bind to Fe-, Al- and Ti-(oxyhydr)oxides (Gustafsson 2019), thus causing the interpretation of the observed V-enrichment patterns and pathways to be challenging. Furthermore, V(IV) reduction to V(III) and sorption to clay minerals have been shown to occur under strongly reducing conditions in sediments facilitated by the presence of H_2S (Scott et al. 2017). Such V(III) could substitute octahedral positions in the clay mineral crystals (Breit & Wanty 1991; Gustafsson 2019) and the vana-diferous illitic illite-smectite has been reported from V-rich black shales (Peacor et al. 2000). Vanadium incorporated into clay minerals could have been originally scavenged by OM and afterwards redistributed within sediments. Still, the data gathered from the Sõtke section indicate that V accumulation in sediments was first of all determined by mineral matter rather than OM. The observed co-variance between V and OM might, on the other hand, just reflect combined sedimentation (formation of organic–clay mineral flocs in the water column; e.g., Schieber et al. 2007) or preservation (protection of organic matter by a mineral matrix; e.g., Salmon et al. 2000) pathways of organics and fine-grained mineral matter. Overall, the data gathered from the Sõtke black shale profile seem to be in accordance with V scavenging from the water column by high-surface-area mineral matter or organic–mineral flocs and vanadiferous phyllosilicates occurring via prime carriers of the metal in the rock.

Uranium

Kochenov & Baturin (2002) suggested that the association of U with phosphate phases (U has a strong affinity towards P) explains its particularly high enrichment in the Türisalu Formation of NE Estonia. They further estimated that 30–40% of U stays phosphate-bonded, whereas 20–30% of U is associated with OM. Relying on microanalyses data, Schulz et al. (2019) recently reported that elevated U in contemporaneous black shales from the St Petersburg region tended to be associated with detrital apatite, Ti-oxides and graptolite fragments.

The elevated U content in the black shales of the lower part of the Sõtke section most likely reflects the input of

detrital phosphates, as the U-rich interval comprises coarse-grained black shales containing bioclastic apatite. Uranium enrichment in biogenic detrital apatite could take place over several sedimentation–denudation cycles of the mud beds. Furthermore, opened porosity in such P-rich beds and more active hydrodynamic conditions could have been critical for enhanced U transfer across the sediment–water interface (e.g., Schovsbo 2002).

Nevertheless, the lack of significant covariance between recorded U and P, as well as between U and TOC, suggests multivariate control over U-enrichment. The behaviour of U is sensitive to a complex set of factors, including Eh and pH changes and the presence of complexing ligands and OM (Cumberland et al. 2016). Uranium enrichment in organic-rich sediments is thought to proceed mainly through the abiotic or biotic reduction of U(VI) to U(IV) within the sediment column, whereas reduced species are either retained in sediments via uraninite or adsorbed by OM in the presence of aqueous H_2S complexes (Bone et al. 2017). Under higher Eh, more basic pH and the presence of dissolved carbonate, U(VI) is expected to form soluble uranyl carbonate complexes. In sediments with circumneutral pH and with a low content of dissolved carbonates and a high content of phosphorus species, poorly soluble uranyl phosphates are likely to form, supporting U entrapment within the solid matter (Cumberland et al. 2016). The presence of early post-depositional authigenic phosphates within U-enriched intervals of the studied black shales points to high dissolved phosphorus in the primary sediment. The precipitation of authigenic phosphates within the uppermost sedimentary column near the suboxic–anoxic boundary could be triggered by sulphate reduction and coupled P liberation, as demonstrated by studies of modern marine sediments (März et al. 2018). The phosphate saturation in sediment pore water and spontaneous precipitation of Ca-phosphate could have been controlled by the presence of polyphosphates containing sulphur bacteria at or near the sediment–water interface. Release of phosphates by such sulphide-oxidizing bacteria is thought to be the major driving force behind the accumulation of modern sedimentary phosphorites under biologically highly productive areas on continental shelves (Schulz & Schulz 2005).

Notably, the production of CO_3^{2-} in the sulphate reduction zone might have aided the solubilization of U and led to preferential sequestration of U into phosphate-rich horizons. Such U-enrichment scenarios fit well with geochemical patterns in the upper part of the black shale sequence of the Sõtke core, where the U–P-rich interval is overlying carbonate-rich horizons. The latter could be relicts of intensive sulphate reduction zones in the primary sedimentary column.

Phosphate minerals may also scavenge U from groundwater over a prolonged period during diagenesis (Kochenov & Baturin 2002), while reduced U in organic-rich sediments could also be remobilized by oxidation. Thus, Schulz et al. (2019) suggested that Tremadocian black shales of this region experienced a considerable mass transfer of U during the last ice ages due to the flushing of the permeable layers of the complex by oxygen-rich glacier meltwater. Still, it is not clear to what extent the processes mentioned above may have affected the development of the observed U distribution.

Zinc and lead

Zinc may demonstrate a non-conservative behaviour in a productive water column due to scavenging by organic particles (Kunzmann et al. 2019). However, Zn–Pb mineralization in sediments could also be associated with the syngenetic exhalative hydrothermal fluids. Petersell et al. (1987) suggested, on the basis of pyrite $\delta^{34}S$ data (for which they reported a main variation range of $\delta^{34}S$ to be from +2.9‰ to –3.8‰), that the enrichment of chalcophile metals in the Türisalu Formation had been triggered by the influx of hydrothermal fluids to the sea basin. However, the lack of evidence that could verify simultaneous volcanic activity in the Baltic Palaeobasin makes such a scenario questionable. On the other hand, Estonian Palaeozoic carbonate complexes do contain scattered Pb and Zn mineralization, which has been attributed to the influx of middle Devonian saline NaCl–$CaCl_2$–H_2O basinal brines (Eensaar et al. 2017). The Sõtke borehole is located in the proximity of the Sirgala tectonic dislocation, which shows widespread dolomitic alteration and is thought to have evolved due to distal stresses of the Caledonian orogeny (Puura & Vaher 1997). It is thus likely that the Pb–Zn mineralization in black shales of the Sillamäe area was triggered by the flow of pressurized saline fluids discharged from the Sirgala dislocation. Judging from the gathered geochemical data, the presence of authigenic carbonate phases seems to be critical for Zn-enrichment, hinting that calcite dissolution likely preceded the entrapment of metals generating secondary porosity, which supported sphalerite precipitation (e.g., Leach et al. 2006). The primary source(s) of Zn and Pb for such fluids could have been Zn–Pb-rich Palaeoproterozoic basement complexes of NE Estonia (Puura & Sudov 1976) or redistribution of syngenetically trapped metals by percolating saline fluids.

CONCLUSIONS

Polymetallic mineralization in Tremadocian black shales in the Sillamäe area evolved as a combined result of

syngenetic and epigenetic processes under a semi-open geochemical system. While high bioproduction and low Eh in the benthic zone were prerequisites for syngenetic U, Mo and V accumulation, the development of the observed distribution patterns of the metals was strongly controlled by local physical features of primary mud complexes. The compartmentalized anisotropic architecture of the mud sequences with high-permeability interlayers helped in creating steep redox gradients in shallow pore water. The development of an intensive sulphide reduction zone with rapid labile OM mineralization and H_2S production, which also triggered major alkalinity and pH shifts and carbonate precipitation near the sediment–water interface, was likely the key factor for locally enhanced Mo entrapment. The input of detrital phosphate phases and phosphorus redistribution in mud deposited near the redoxcline were critical for U mineralization in most U-enriched intervals. The carbonate-rich black shales studied in the Sillamäe area probably behaved as a complex geochemical trap during late diagenesis, capturing Zn and Pb from epigenetic metal-bearing basinal brines.

Supplementary online data

Supplementary material to this article is available online at https://doi.org/10.15152/GEO.500, presenting an image of the black shale section of the Sõtke core. The full geochemical dataset for the black shales of the Sõtke core is provided at https://doi.org/10.15152/GEO.499.

REFERENCES

Algeo, T. J. & Lyons, T. W. 2006. Mo-total organic carbon covariation in modern anoxic marine environments: Implications for analysis of paleoredox and paleohydrographic conditions. *Paleoceanography*, **21**, PA1016.

Algeo, T. J. & Maynard, J. B. 2004. Trace-element behavior and redox facies in core shales of Upper Pennsylvanian Kansas-type cyclothems. *Chemical Geology*, **206**, 289–318.

Algeo, T. J. & Tribovillard, N. 2009. Environmental analysis of paleoceanographic systems based on molybdenum–uranium covariation. *Chemical Geology*, **268**, 211–225.

Andersson, A., Dahlman, B., Gee, D. G. & Snäll, S. 1985. The Scandinavian Alum Shales. *Sveriges Geologiska Undersökning, Serie Ca*, 56, 1–52.

Artyushkov, E. A., Lindström, M. & Popov, L. E. 2000. Relative sea-level changes in Baltoscandia in the Cumbrian and early Ordovician: the predominance of tectonic factors and the absence of large scale eustatic fluctuations. *Tectonophysics*, **320**, 375–407.

Baturin, G. N. & Ilyin, A. V. 2013. Comparative geochemistry of shell phosphorites and dictyonema shales of the Baltic. *Geochemistry International*, **51**, 23–32.

Bogdanov, R., Ozernaja, S., Pihlak, A. & Lippmaa, E. 1994. The detection of the markedly depleted in U-234 Dictyoneme shale component. *Geokhimiya*, **11**, 1626–1632 [in Russian, with English summary].

Bogdanov, R., Ozernaja, S., Pihlak, A.-T. & Timofeev, S. 2007. Radiogenic uranium-234 in humus acids of graptolitic argillite. *Oil Shale*, **24**, 73–89.

Bone, S. E., Dynes, J. J., Cliff, J. & Bargar, J. R. 2017. Uranium(IV) adsorption by natural organic matter in anoxic sediments. *Proceedings of the National Academy of Sciences of the United States of America*, **114**, 711–716.

Breit, G. N. & Wanty, R. B. 1991. Vanadium accumulation in carbonaceous rocks: A review of geochemical controls during deposition and diagenesis. *Chemical Geology*, **91**, 83–97.

Cocks, L. R. M. & Torsvik, T. H. 2006. European geography in a global context from the Vendian to the end of the Palaeozoic. *Geological Society, London, Memoirs*, **32**, 83–95.

Coveney, R. M. & Nansheng, C. 1991. Ni-Mo-PGE-Au-rich ores in Chinese black shales and speculations on possible analogues in the United States. *Mineralium Deposita*, **26**, 83–88.

Cumberland, S. A., Douglas, G., Grice, K. & Moreau, J. W. 2016. Uranium mobility in organic matter-rich sediments: A review of geological and geochemical processes. *Earth-Science Reviews*, **159**, 160–185.

Dellwig, O., Leipe, T., März, C., Glockzin, M., Pollehne, F., Schnetger, B., Yakushev, E. V., Böttcher, M. E. & Brumsack, H. J. 2010. A new particulate Mn-Fe-P-shuttle at the redoxcline of anoxic basins. *Geochimica et Cosmochimica Acta*, **74**, 7100–7115.

Deng, Y., Chen, F., Hu, Y., Guo, Q., Cao, J., Chen, H., Zhou, J., Jiang, X. & Zhu, J. 2020. Methane seepage patterns during the middle Pleistocene inferred from molybdenum enrichments of seep carbonates in the South China Sea. *Ore Geology Reviews*, **125**, 103701.

Eensaar, J., Gaškov, M., Pani, T., Sepp, H., Somelar, P. & Kirsimäe, K. 2017. Hydrothermal fracture mineralization in the stable cratonic northern part of the Baltic Paleobasin: sphalerite fluid inclusion evidence. *GFF*, **139**, 52–62.

Eichwald, C. E. von. 1840. *Ueber das silurische Schichtensystem in Esthland*. Medizinischen Akademie, St. Petersburg, 210 pp.

Erickson, B. E. & Helz, G. R. 2000. Molybdenum(VI) speciation in sulfidic waters. *Geochimica et Cosmochimica Acta*, **64**, 1149–1158.

Felitsyn, S. B., Vidal, G. & Moczydłowska, M. 1998. Trace elements and Cr and C isotopic signatures in late Neoproterozoic and earliest Cambrian sedimentary organic

matter from siliciclastic successions in the East European Platform. *Geological Magazine*, **135**, 537–551.

Gill, B. C., Lyons, T. W., Young, S. A., Kump, L. R., Knoll, A. H. & Saltzman, M. R. 2011. Geochemical evidence for widespread euxinia in the Later Cambrian ocean. *Nature*, **469**, 80–83.

Guilbaud, R., Slater, B., Poulton, S., Harvey, T., Brocks, J., Nettersheim, B. & Butterfield, N. 2017. Oxygen minimum zones in the early Cambrian ocean. *Geochemical Perspectives Letters*, **6**, 33–38.

Gustafsson, J. P. 2019. Vanadium geochemistry in the biogeosphere – speciation, solid-solution interactions & ecotoxicity. *Applied Geochemistry*, **102**, 1–25.

Hade, S. & Soesoo, A. 2014. Estonian graptolite argillites revisited. A future resource? *Oil Shale*, **31**, 4–18.

Heinsalu, H. N. 1987. Lithostratigraphical subdivision of Tremadoc deposits of North Estonia. *Proceedings of the Academy of Sciences of the Estonian SSR, Geology*, **36**, 66–78 [in Russian, with English summary].

Heinsalu, H. & Bednarczyk, W. 1997. Tremadoc of the East European Platform: lithofacies and palaeogeography. *Proceedings of the Estonian Academy of Sciences, Geology*, **46**, 59–74.

Heinsalu, H., Kaljo, D., Kurvits, T. & Viira, V. 2003. The stratotype of the Orasoja Member (Tremadocian, Northeast Estonia): lithology, mineralogy, and biostratigraphy. *Proceedings of the Estonian Academy of Sciences, Geology*, **52**, 135–154.

Helz, G. R. & Vorlicek, T. P. 2019. Precipitation of molybdenum from euxinic waters and the role of organic matter. *Chemical Geology*, **509**, 178–193.

Helz, G. R., Miller, C. V., Charnock, J. M., Mosselmans, J. F. W., Pattrick, R. A. D., Garner, C. D. & Vaughan, D. J. 1996. Mechanism of molybdenum removal from the sea and its concentration in black shales: EXAFS evidence. *Geochimica et Cosmochimica Acta*, **60**, 3631–3642.

Hints, R., Hade, S., Soesoo, A. & Voolma, M. 2014. Depositional framework of the East Baltic Tremadocian black shale revisited. *GFF*, **136**, 464–482.

Johnson, S. C., Large, R. R., Coveney, R. M., Kelley, K. D., Slack, J. F., Steadman, J. A., Gregory, D. D., Sack, P. J. & Meffre, S. 2017. Secular distribution of highly metalliferous black shales corresponds with peaks in past atmosphere oxygenation. *Mineralium Deposita*, **52**, 791–798.

Jones, B. & Manning, D. A. C. 1994. Comparison of geochemical indices used for the interpretation of palaeoredox conditions in ancient mudstones. *Chemical Geology*, **111**, 111–129.

Kaljo, D. & Kivimägi, E. 1970. On the distribution of graptolites in the dictyonema shale of Estonia and on the uncontemporaneity of its different facies. *Eesti NSV Teaduste Akadeemia Toimetised, Keemia, Geoloogia*, **19**, 334–341 [in Russian, with English summary].

Kallaste, T. & Pukkonen, E. 1992. Pyrite varieties in Estonian Tremadocian argillite (Dictyonema shale). *Proceedings of the Estonian Academy of Sciences, Geology*, **41**, 11–22.

Karimov, M., Petersell, V. & Tarros, S. 2017. *Puuraugu rajamine Sõtke uuringuruumis* [*Making a Borehole in the Sõtka Study Area*]. Unpublished report, Eesti Geoloogiakeskus, Tallinn, 25 pp. [in Estonian].

Kiipli, T., Batchelor, R. A., Bernal, J. P., Cowing, C., Hagel-Brunnstrom, M., Ingham, M. N., Johnson, D., Kivisilla, J., Knaack, C., Kump, P., Lozano, R., Michiels, D., Orlova, K. & Pirrus, E. 2000. Seven sedimentary rock reference samples from Estonia. *Oil Shale*, **17**, 215–223.

Kirsimäe, K., Jørgensen, P. & Kalm, V. 1999. Low-temperature diagenetic illite-smectite in Lower Cambrian clays in North Estonia. *Clay Minerals*, **34**, 151–163.

Kochenov, A. V. & Baturin, G. N. 2002. The paragenesis of organic matter, phosphorus, and uranium in marine sediments. *Lithology and Mineral Resources*, **37**, 107–120.

Kunzmann, M., Schmid, S., Blaikie, T. N. & Halverson, G. P. 2019. Facies analysis, sequence stratigraphy, and carbon isotope chemostratigraphy of a classic Zn-Pb host succession: The Proterozoic middle McArthur Group, McArthur Basin, Australia. *Ore Geology Reviews*, **106**, 150–175.

Leach, D., Macquar, J.-C., Lagneau, V., Leventhal, J., Emsbo, P. & Premo, W. 2006. Precipitation of lead–zinc ores in the Mississippi Valley-type deposit at Trèves, Cévennes region of southern France. *Geofluids*, **6**, 24–44.

Leventhal, J. S. 1983. An interpretation of carbon and sulfur relationships in Black Sea sediments as indicators of environments of deposition. *Geochimica et Cosmochimica Acta*, **47**, 133–137.

Lippmaa, E., Maremäe, E., Pihlak, A.-T. & Aguraiuja, R. 2009. Estonian graptolitic argillites – ancient ores or future fuels? *Oil Shale*, **26**, 530–539.

Lippmaa, E., Maremäe, E. & Pihlak, A.-T. 2011. Resources, production and processing of Baltoscandian multimetal black shales. *Oil Shale*, **28**, 68–77.

Loog, A., Kurvits, T., Aruväli, J. & Petersell, V. 2001. Grain size analysis and mineralogy of the Tremadocian Dictyonema shale in Estonia. *Oil Shale*, **18**, 281–297.

März, C., Riedinger, N., Sena, C. & Kasten, S. 2018. Phosphorus dynamics around the sulphate-methane transition in continental margin sediments: Authigenic apatite and Fe(II) phosphates. *Marine Geology*, **404**, 84–96.

Mikhailova, K., Vasileva, K., Fedorov, P., Ershova, V., Vereshchagin, O., Rogov, M. & Pokrovsky, B. 2019. Glendonite-like carbonate aggregates from the Lower Ordovician Koporye Formation (Russian Part of the Baltic Klint): Detailed mineralogical and geochemical data and paleogeographic implications. *Minerals*, **9**, 524.

Morford, J. L., Martin, W. R., Kalnejais, L. H., François, R., Bothner, M. & Karle, I.-M. 2007. Insights on geochemical cycling of U, Re and Mo from seasonal sampling in Boston Harbor, Massachusetts, USA. *Geochimica et Cosmochimica Acta*, **71**, 895–917.

Nielsen, A. T. & Schovsbo, N. H. 2006. Cambrian to basal Ordovician lithostratigraphy in Southern Scandinavia. *Bulletin of the Geological Society of Denmark*, **53**, 47–92.

Pagès, A., Barnes, S., Schmid, S., Coveney, R. M., Schwark, L., Liu, W., Grice, K., Fan, H. & Wen, H. 2018. Geochemical investigation of the lower Cambrian mineralised black shales of South China and the late Devonian Nick deposit, Canada. *Ore Geology Reviews*, **94**, 396–413.

Peacor, D. R., Coveney, R. M. & Zhao, G. 2000. Authigenic illite and organic matter: The principal hosts of vanadium in the

Mecca Quarry Shale at Velpen, Indiana. *Clays and Clay Minerals*, **48**, 311–316.

Petersell, V. 1997. *Dictyonema* argillite. In *Geology and Mineral Resources of Estonia* (Raukas, A. & Teedumäe, A., eds), pp. 327–331. Estonian Academy Publishers, Tallinn.

Petersell, V. H., Zhukov, F. I., Loog, A. R. & Fomin, Y. A. 1987. Origin of Tremadoc kerogen-bearing siltstones and argillites of North Estonia. *Oil Shale*, **4**, 7–13 [in Russian, with English summary].

Popov, L. E., Álvaro, J. J., Holmer, L. E., Bauert, H., Ghobadi Pour, M., Dronov, A. V., Lehnert, O., Hints, O., Männik, P., Zhang, Z. & Zhang, Z. 2019. Glendonite occurrences in the Tremadocian of Baltica: first Early Palaeozoic evidence of massive ikaite precipitation at temperate latitudes. *Scientific Reports*, **9**, 7205.

Pukkonen, E. 1989. Major and minor elements in Estonian graptolite argillite. *Oil Shale*, **6**, 11–18.

Puura, V. & Sudov, B. 1976. The tectonically active platform zones on the south slope of the Baltic shield and their metallogeny. *Eesti NSV Teaduste Akadeemia Toimetised, Keemia, Geoloogia*, **25**, 206–214 [in Russian, with English summary].

Puura, V. & Vaher, R. 1997. Cover structure. In *Geology and Mineral Resources of Estonia* (Raukas, A. & Teedumäe, A., eds), pp. 167–177. Estonian Academy Publishers, Tallinn.

Salmon, V., Derenne, S., Lallier-Vergès, E., Largeau, C. & Beaudoin, B. 2000. Protection of organic matter by mineral matrix in a Cenomanian black shale. *Organic Geochemistry*, **31**, 463–474.

Schieber, J. & Riciputi, L. 2005. Pyrite and marcasite coated grains in the Ordovician Winnipeg Formation, Canada: An intertwined record of surface conditions, stratigraphic condensation, geochemical "reworking", and microbial activity. *Journal of Sedimentary Research*, **75**, 907–920.

Schieber, J., Southard, J. B. & Thaisen, K. 2007. Accretion of mudstone beds from migrating floccule ripples. *Science*, **318**, 1760–1763.

Schlanger, S. O., Arthur, M. A., Jenkyns, H. C. & Scholle, P. A. 1987. The Cenomanian-Turonian Oceanic Anoxic Event, I. Stratigraphy and distribution of organic carbon-rich beds and the marine δ^{13}C excursion. *Geological Society Special Publication*, **26**, 371–399.

Schlesinger, W. H., Klein, E. M. & Vengosh, A. 2017. Global biogeochemical cycle of vanadium. *Proceedings of the National Academy of Sciences of the United States of America*, **114**, E11092–E11100.

Scholz, F., Baum, M., Siebert, C., Eroglu, S., Dale, A. W., Naumann, M. & Sommer, S. 2018. Sedimentary molybdenum cycling in the aftermath of seawater inflow to the intermittently euxinic Gotland Deep, Central Baltic Sea. *Chemical Geology*, **491**, 27–38.

Schovsbo, N. H. 2002. Uranium enrichment shorewards in black shales: A case study from the Scandinavian Alum Shale. *GFF*, **124**, 107–115.

Schulz, H.-M., Yang, S., Panova, E. & Bechtel, A. 2019. The role of Pleistocene meltwater-controlled uranium leaching in assessing irradiation-induced alteration of organic matter and petroleum potential in the Tremadocian Koporie Formation (Western Russia). *Geochimica et Cosmochimica Acta*, **245**, 133–153.

Schulz, H. N. & Schulz, H. D. 2005. Large sulfur bacteria and the formation of phosphorite. *Science*, **307**, 416–418.

Scott, C. & Lyons, T. W. 2012. Contrasting molybdenum cycling and isotopic properties in euxinic versus non-euxinic sediments and sedimentary rocks: Refining the paleoproxies. *Chemical Geology*, **324–325**, 19–27.

Scott, C., Slack, J. F. & Kelley, K. D. 2017. The hyper-enrichment of V and Zn in black shales of the Late Devonian-Early Mississippian Bakken Formation (USA). *Chemical Geology*, **452**, 24–33.

Scranton, M. I., Sayles, F. L., Bacon, M. P. & Brewer, P. G. 1987. Temporal changes in the hydrography and chemistry of the Cariaco Trench. *Deep Sea Research Part A. Oceanographic Research Papers*, **34**, 945–963.

Smedley, P. L. & Kinniburgh, D. G. 2017. Molybdenum in natural waters: A review of occurrence, distributions and controls. *Applied Geochemistry*, **84**, 387–432.

Sturesson, U. L. F., Popov, L. E., Holmer, L. E., Bassett, M. G., Felitsyn, S. & Belyatsky, B. 2005. Neodymium isotopic composition of Cambrian–Ordovician biogenic apatite in the Baltoscandian Basin: implications for palaeogeographical evolution and patterns of biodiversity. *Geological Magazine*, **142**, 419–439.

Taylor, S. R. & McLennan, S. M. 1985. *The Continental Crust: Its Composition and Evolution. An Examination of the Geochemical Record Preserved in Sedimentary Rocks.* Blackwell Science, Oxford, 312 pp.

Thickpenny, A. 1984. The sedimentology of the Swedish Alum Shales. *Geological Society, London, Special Publications*, **15**, 511–525.

Tribovillard, N., Algeo, T. J., Lyons, T. W. & Riboulleau, A. 2006. Trace metals as paleoredox and paleoproductivity proxies: An update. *Chemical Geology*, **232**, 12–32.

Tyson, R. V. 2001. Sedimentation rate, dilution, preservation and total organic carbon: some results of a modelling study. *Organic Geochemistry*, **32**, 333–339.

Utsal, K., Kivimägi, E. & Utsal, V. 1980. About the method of investigating Estonian graptolithic argillite and its mineralogy. *Tartu Riikliku Ülikooli Toimetised*, **527**, 116–138 [in Russian, with English summary].

Vind, J. & Bauert, H. 2020. *Geochemical Characterisation of the Tremadocian Black Shale in North-Western Estonia.* No. EGF9330. Geological Survey of Estonia, Rakvere, 91 pp.

Wignall, P. B. & Newton, R. 2001. Black shales on the basin margin: A model based on examples from the Upper Jurassic of the Boulonnais, Northern France. *Sedimentary Geology*, **144**, 335–356.

Wilde, P., Quinby-Hunt, M. S., Berry, W. B. N. & Orth, C. J. 1989. Palaeo-oceanography and biogeography in the Tremadoc (Ordovician) Iapetus Ocean and the origin of the chemostratigraphy of *Dictyonema flabelliforme* black shales. *Geological Magazine*, **126**, 19–27.

Wilde, P., Lyons, T. W. & Quinby-Hunt, M. S. 2004. Organic carbon proxies in black shales: Molybdenum. *Chemical Geology*, **206**, 167–176.

Zhao, M. Y., Zheng, Y. F. & Zhao, Y. Y. 2016. Seeking a geochemical identifier for authigenic carbonate. *Nature Communications*, **7**, 1–7.

Metallide rikastumine litoloogiliselt komplekssetes Tremadoci mustades kiltades Kirde-Eestis

Rutt Hints, Siim Pajusaar, Kristjan Urtson, Merilin Liiv ja Toivo Kallaste

On käsitletud Balti Paleobasseini mustade kiltade metallogeneesi, keskendudes Sillamäe piirkonna metallirikka graptoliitargilliidi läbilõigetele. Rohkete sulfiidistunud aleuroliidi vahekihtide ja autigeensete karbonaatide levik eristab sealseid graptoliitargilliidi läbilõikeid tüüpilistest litoloogiliselt homogeensematest mustadest kiltadest. Graptoliitargilliidi elementkoostise leviku detailkaardistamiseks Sõtke puuraugu ja Päite klindi läbilõikes kasutati röntgenfluorestsentsanalüüsi, induktiivsidestatud plasma massispektromeetriat ning orgaanilise aine elementanalüüsi. Valitud proove uuriti täiendavalt valgus- ja elektronmikroskoopiaga ning energiadispersiivsel röntgenmikroanalüüsil. Rikastunud metallide sisaldused graptoliitargilliidis olid U 88–275 ppm, Mo 70–2467 ppm, V 85–1600 ppm, Zn 21–17 283 ppm ja Pb 95–26 549 ppm ning kogu orgaanilise süsiniku sisaldus oli 0,5–13%. Metallide leviku heterogeensus viitab komplekssete muutujate rollile nende akumuleerumisprotsessis. Mo rikastumine peegeldab tõenäoliselt intensiivse sulfaatide redutseerumise tsooni kujunemist orgaanikarikaste mudade ülakihis, millega kaasnesid suur H_2S kontsentratsioon, leelisus ja pH poorivees. Osa rikastunud U-d seoti süngeneetiliselt autigeensetesse ja detriitsetesse fosfaatsetesse faasidesse. Metallide rikastumist Sillamäe piirkonna graptoliitargilliidis soodustas setendi keskmisest suurem geokeemiline avatus. Lokaalne Zn ja Pb rikastumine kujunes hilisdiageneetiliste metallirikaste fluidide tungimisel graptoliitargilliiti ning metallide sidumisel karbonaate sisaldavates kivimikihtides.